Mater. Res. Soc. Symp. Proc. Vol. 1446 © 2012 Materials Research Society
DOI: 10.1557/opl.2012.1249

Hydrogen Generation for 500 hours by Photoelectrolysis of Water using GaN

W. Ohara, D. Uchida, T. Hayashi, M. Deura, and K. Ohkawa
Department of Applied Physics, Tokyo University of Science, 1-3 Kagurazaka, Shinjuku, Tokyo 162-8601, Japan

ABSTRACT

We confirmed that GaN photocatalyst with NiO cocatalyst (GaN-NiO) continuously produced hydrogen from water for 500 hours without any extra bias. The GaN-NiO photocatalyst was hardly etched and 184-mL hydrogen gas was produced from the electric charge of 1612 coulombs, the Faradic efficiency of which was 89.2%. The conversion efficiency from incident light energy to hydrogen chemical energy was 0.98% in average for 500 h. The incident photon-to-current conversion efficiency (IPCE) was 50% at 300 nm and 35% at 350 nm after the experiment, which was much higher than those of other semiconductor-based photocatalysts.

INTRODUCTION

Since no CO_2 is discharged after its combustion, hydrogen is promising as the new energy source instead of fossil fuels. As a method of H_2 generation, photoelectrolysis of water using photocatalysts is attracting because only water and solar light energy are necessary [1-5].

We have focused on III-nitrides, especially GaN, as the photocatalyst [6-14]. Their band edge potentials are comparatively higher than those of conventional oxides used as photocatalysts and straddle the oxidation-reduction level of water. In fact, we have realized H_2 generation using GaN photocatalyst without any extra bias. Moreover, they can absorb not only ultraviolet but also visible light using InGaN alloys by changing the group-III content.

However, most of the photocatalysts have insufficient durability for practical use. Although GaN is chemically stable essentially, GaN layer itself is etched during photocatalytic reaction due to holes generated by light illumination and accumulated on the surface of the GaN layer. This etching reduces the durability of the photocatalyst. We have found that deposition of NiO cocatalyst on the GaN layer avoids the etching [15]. Furthermore, the amount of H_2 generated for GaN photocatalyst with NiO (GaN-NiO) increased more than four times compared to that for GaN (GaN w/o NiO). In this study, we investigated the stability of hydrogen generation from water using GaN-NiO for 500 hours.

EXPERIMENT

We used a 3-μm-thick n-type GaN layer on a sapphire substrate grown by metalorganic vapor-phase epitaxy, and NiO was deposited with around 1.2% coverage on the GaN surface. The film thickness of GaN was 3.1μm, and its room temperature carrier density and electron

mobility were 1.2×10^{17} cm^{-3} and 580 $cm^2/V\cdot s$, respectively. This GaN-NiO working electrode connected to the Pt counterelectrode was dipped into a NaOH solution with the concentration of 1 mol/L. The irradiated area of the GaN-NiO electrode was adjusted to 1.0 cm^2 by covering the remaining area with epoxy resin. A Xe lamp with the energy density of 100 mW/cm^2 was used as the light source and the photocurrent density was measured using a potentiostat. All of the experiments were performed at room temperature, and no bias was applied to this system. We conducted 500 h experiment with 50 repetitions of a 10 h experiment. We measured the amount of generated H_2, the energy conversion efficiency, the incident photon-to-current conversion efficiency (IPCE), and change in the surface of the GaN layer.

DISCUSSION

Time evolution of the amount of hydrogen

Time evolution of the amount of generated hydrogen for 500 hours is shown in Fig. 1. The amount was increased gradually until 60h. This may be due to the oxidation of epoxy resin instead of O_2 generation [16]. Drastic drop between 110 and 120 h is caused by degradation of the intensity of the Xe lamp. In fact, the amount was recovered after the lamp was exchanged after 480h. Therefore, the decrease at120 h is not due to the deterioration of the GaN-NiO electrode. Since the amount of generated H_2 was stable between 120 to 480 h, the function as the photocatalyst retained for 500 h. Total amount of H_2 produced for 500 h was 184 mL from the electric charge of 1612 C, and thus the Faradic efficiency (electric charges used for hydrogen generation/ generated electric charges) was 89.2%. This amount of generated H_2 corresponds to 37 $mL/cm^2/100$ h, which is over one magnitude larger than that for Cu_2O (1.6×10^{-4} $mL/cm^2/100$ h) [17] or $NiO/NaTaO_3$:La (2.2 $mL/cm^2/100$ h) [18].

The surface morphology of the GaN-NiO and GaN w/o NiO electrode was observed by a Nomarski microscope as shown in Fig.2. A lot of dark points were observed over the entire surface of GaN w/o NiO after the experiment. All of these points were pits, which were measured by a stylus surface profiler. The value of RMS (root mean square) of the surface roughness was 101 nm, which was 100 times larger than that before the experiment. Ga, N, and

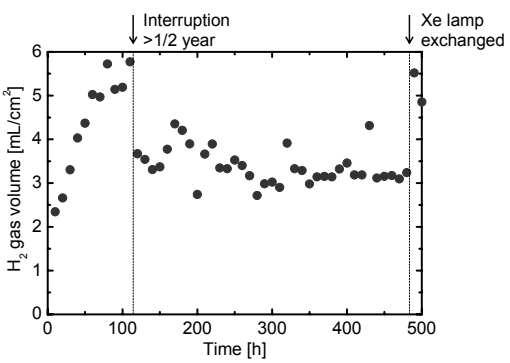

Figure 1. Time evolution of generated hydrogen for 500 hours.

O were detected in the points by energy dispersive X-ray spectrometry (EDS). Therefore, the dark points were due to the etching of the surface. In contrast, the GaN-NiO surface was not clearly changed even after 500 h, and the RMS of the roughness was 9.3 nm. Although a few dark points were observed on the surface as shown in Fig. 2(b), the amount of generated H_2 was constant; this is because ratio of the degraded area was small compared to the whole surface area. Some of these points were not pits but projections. Since the C peak was detected in addition to the Ga, N, and O peaks in the dark points of GaN-NiO, the projected points were maybe attributed to some organic decomposition from such as epoxy resin.

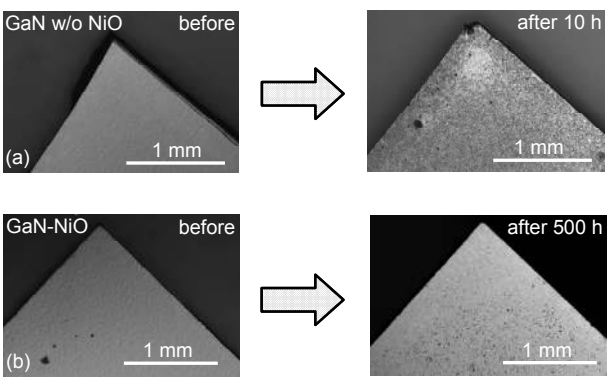

Figure 2. The surface morphology of the (a) GaN w/o NiO and (b) GaN-NiO electrode observed by a Nomarski microscope.

Energy conversion efficiency

The energy conversion efficiency from incident light energy to hydrogen chemical energy was described by Eq. 1.

$$\text{Energy convertion efficiency} = \frac{\text{Hydrogen energy}}{\text{Incidence light energy}} = \frac{\Delta G^0 \times n}{P \times A \times t} \quad (1)$$

where $\Delta G°$=237 kJ/mol is the Gibbs energy of H_2 combustion, n is the number of hydrogen molecules, P is the incident light intensity, A is the area of light illumination, and t is time. In the case of the GaN-NiO photocatalyst, this efficiency was 1.54% in maximum (100-110 h) and 0.98% in average for 500 h. This efficiency was 4.6 times larger than that for GaN w/o NiO of 0.33%.

Figure 3 is the IPCE of the GaN-NiO photocatalyst before and after the 500 h experiment. We used a monochromatic light with full-width at half maximum of 2.8 nm at 350 nm from a Xe lamp using a monochromator, and incident light energy to the GaN surface was a few hundred

μW. IPCE is the conversion efficiency from the number of photons to the number of electrons produced as defined in Eq. 2.

$$\text{IPCE} = \frac{\text{number of electrons produced}}{\text{number of incident photons}} = \frac{I_P/e}{P \times \lambda/hc} \quad (2)$$

where I_P is the photocurrent density, e is the elementary electric charge, P is the power density of monochromatic light, λ is wavelength of the incident light, h is the Planck's constant, and c is the speed of light in vacuum. IPCE is decreased rapidly above near 360 nm corresponding to 3.42 eV (363 nm) of the bandgap of GaN. ICPE was 50% at 300 nm and 35% at 350 nm, and these values were much higher than other semiconductor-based photocatalysts.

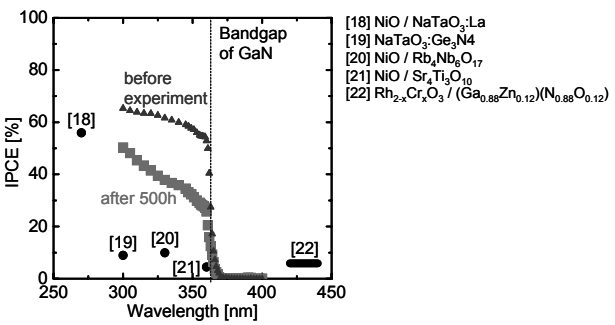

Figure 3. The IPCE of the GaN-NiO photocatalyst before and after the 500 h experiment.

CONCLUSIONS

We investigated the durability of hydrogen generation from water using the GaN-NiO photocatalyst. GaN-NiO produced H_2 continuously with high Faradic efficiency for 500 h without heavy etching. The amount of generated H_2 was over one magnitude larger than that using other materials. The energy conversion efficiency and the ICPE were both distinctly higher than those for other photocatalysts. In conclusion, GaN-NiO works as the photocatalyst for hydrogen generation from water with high efficiency and good stability.

REFERENCES

1. A. Fujishima and K. Honda, Nature **238**, 37 (1972).
2. D. Jing, L. Guo, L. Zhao, X. Zhang, H. Liu, M. Li, S. Shen, G. Liu, X. Hu, X. Zhang, K. Zhang, L. Ma, P. Guo, Int. J. Hydrogen Energy **35**, 7087 (2010).
3. B.Kraeutler and A. J. Bard, J. Am. Cham. Soc. **100**, 4317 (1978).
4. R. Memming, *Semiconductor Electrochemistry*, WILEY-VCH, p. 105 (2001).

5. S. S. Kocha, M. W. Peterson, D. J. Arent, J. M. Redwing, M. A. Tischler, J. A. Turner, J. Electrochem. Soc. **142**, L236 (1995).
6. M. Ono, K. Fujii, T. Ito, Y. Iwaki, T. Yao, K. Ohkawa, J. Chem. Phys. **126**, 054708 (2007).
7. K. Fujii and K. Ohkawa, Jpn. J. Appl. Phys. **44**, L909 (2005).
8. K. Fujii, K. Kusakabe, K. Ohkawa, Jpn. J. Appl. Phys. **44**, 7433 (2005).
9. K. Fujii and K. Ohkawa, J. Electrochem. Soc. **153**, A468 (2006).
10. K. Fujii and K. Ohkawa, Phys. Status Soldi C **3**, 2270 (2006).
11. K. Fujii, M. Ono, T. Ito, K. Ohkawa, Mater. Res. Soc. Sym. Proc. 0885-A11-04.1 (2006).
12. K. Fujii, T. Ito, M. Ono, Y. Iwaki, T. Yao, K. Ohkawa, Phys. Status Solidi C **4**,2650 (2007).
13. K. Fujii, Y. Iwaki, H. Masui, T. J. Baker. M. Iza, H. Sato, J. Keading, T. Yao, J. S. Speck, S. P. DenBaars, S. Nakamura, K. Ohkawa, Jpn. J. Appl. Phys. **46**, 6573 (2007).
14. K. Fujii, T. Karasawa, K. Ohkawa, Jpn. J. Appl. Phys. **44**, 543 (2005).
15. F. Sano, T. Koyama, M. Sorimachi, A. Hirako, K. Ohkawa, The 8th Int'l Conf. on Nitride Semiconductors, p. 18 (2009).
16. K. Ito, S. Ikeda, M. Yoshida, S. Ohta, and T. Iida, Bull. Chem. Soc. Jpn. **57**, 583 (1984).
17. M. Hara, T. Kondo, M. Komoda, S. Ikeda, K. Shinohara, A. Tanaka, J. N. Kondo, K. Domen, Chem. Commun. **10**, 1039 (1998).
18. H. Kato, K. Asakura, A. Kudo, J. Am. Chem. Soc. **125**, 3082 (2003).
19. H. Kato and A. Kudo, J. Phys. Chem. B **105**, 4285 (2001).
20. K. Sayama and H.Arakawa, Catal. Today **28**, 175 (1997).
21. Y. G. Ko and W. Y. Lee, Catal. Lett. **83**, 157 (2002).
22. K. Maeda, K. Teramura, K. Domen, J. Catal. **254**, 198 (2008).

Mater. Res. Soc. Symp. Proc. Vol. 1446 © 2012 Materials Research Society
DOI: 10.1557/opl.2012.811

Spray-deposited Co-Pi Catalyzed $BiVO_4$: a low-cost route towards highly efficient photoanodes

Fatwa F. Abdi, Nienke Firet, Ali Dabirian and Roel van de Krol
Materials for Energy Conversion and Storage (MECS), Department of Chemical Engineering, Delft University of Technology, P.O. Box 5045, 2600 GA Delft, The Netherlands

ABSTRACT

Bismuth vanadate ($BiVO_4$) thin films are deposited by a low-cost and scalable spray pyrolysis method. Its performance under AM1.5 illumination is mainly limited by slow water oxidation kinetics. We confirm that cobalt phosphate (Co-Pi) is an efficient water oxidation catalyst for $BiVO_4$. The optimum thickness of $BiVO_4$ is 300 nm, resulting in an AM1.5 photocurrent of 1.9 mA/cm^2 at 1.23 V vs. RHE when catalyzed with Co-Pi. Once the water oxidation limitation is removed, the performance is limited by low charge separation efficiency. This causes more than 60% of the electron-hole pairs to recombine before reaching the respective interfaces. The slow electron transport is shown to be the main cause of this low efficiency, and future efforts should therefore be focused on addressing this key limitation.

INTRODUCTION

$BiVO_4$ is considered to be a promising photoanode material for solar water splitting applications. The monoclinic phase has a bandgap of 2.4 eV [1], and can absorb up to 11% of the solar spectrum. Additionally, its conduction band edge is located very close to the reversible hydrogen electrode (RHE) level [2], which enables water splitting at modest external bias potentials. Recent efforts on this material have resulted in significant performance enhancements by the application of oxygen evolution catalysts [3-8]. However, little is known about the factor(s) that limit the performance of $BiVO_4$ after the slow water oxidation kinetics is addressed.

In this study, we use a low-cost spray pyrolysis technique to deposit high-quality $BiVO_4$ films. This technique is highly scalable, an important requirement for large-scale production of solar energy conversion devices. To illustrate this, full conversion to a solar-driven society in 2050, based on 10% efficient devices, requires production rates in the order of 500 m^2/s. This is just one order of magnitude more than the global spray deposition rate in the automotive industry (15 m^2/s). We show that 300 nm is the optimum thickness for our spray-deposited $BiVO_4$ films, resulting in an AM1.5 photocurrent of 1.9 mA/cm^2 at 1.23 V vs. RHE when catalyzed with cobalt phosphate (Co-Pi). This photoanode is limited by a poor charge separation efficiency ($\eta_{sep} < 0.4$), which is caused by the inherently slow electron transport in $BiVO_4$.

EXPERIMENTAL DETAILS

Dense thin films of $BiVO_4$ were prepared by spray pyrolysis, as illustrated in Fig. 1a. A $BiVO_4$ precursor solution was prepared by dissolving $Bi(NO_3)_3.5H_2O$ (98%, Alfa Aesar) in acetic acid (98%, Sigma Aldrich) and $VO(AcAc)_2$ (99%, Alfa Aesar) in absolute ethanol (Sigma Aldrich). The Bi solution was then added to the V solution, and the mixture was diluted to 4 mM with excess ethanol. The substrates are FTO-coated glass (15 Ω/□, TEC-15, Hartford Glass Co.),

which had been cleaned by three successive 15 min. ultrasonic rinsing steps in 10 vol% Triton®, acetone and ethanol. The substrates were placed on a heating plate that was set to 450°C during deposition. The spray nozzle (Quickmist Air Atomizing Spray) was placed 20 cm above the heating plate, and was fed by two nitrogen gas lines (labeled 1 and 2 in Fig. 1) and the liquid $BiVO_4$ precursor solution. Figure 1b shows the schematic representation of the spray nozzle. A pulsed deposition mode was used, with one spray cycle consisting of 5 seconds of spray time and 55 seconds of delay time to allow the solvent to evaporate. In order to prevent large droplets from falling onto the substrate when switching the $BiVO_4$ flow on or off via line 1, gas was flown through line 2 before and after starting and stopping line 1 (Fig. 1c). The thicknesses of $BiVO_4$ were controlled by the number of spray cycles, with a deposition rate of ~1 nm per cycle. Prior to $BiVO_4$ deposition, ~80 nm of SnO_2 layer was deposited onto FTO substrate to prevent recombination of electrons and holes at the FTO/$BiVO_4$ interface [9,10]. After the deposition, the SnO_2/$BiVO_4$ samples were annealed for 2 hours at 450°C in air to further improve the crystallinity.

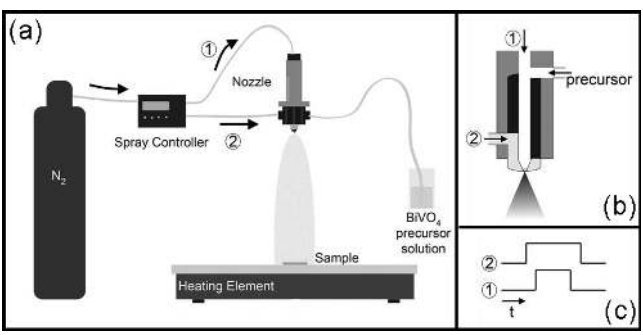

Figure 1. (a) A schematic diagram of the spray pyrolysis setup. The arrows labeled 1 and 2 represent two separate nitrogen flows towards the spray nozzle. (b) A schematic representation of the spray nozzle. (c) Timing of the two separate spray pulses that are supplied to lines 1 and 2.

A 30 nm Co-Pi catalyst was electrodeposited onto the surface of $BiVO_4$ in an electrochemical cell using a three-electrode configuration, according to the recipe from Nocera et al [11]. The electrolyte is made by dissolving 0.5 mM $Co(NO_3)_2$ (99%, Acros Organics) in a 0.1 M KPi solution (pH ~7). The potential of the working electrode was controlled by a potentiostat (EG&G PAR 283). A coiled Pt wire and an Ag/AgCl electrode (XR300, saturated KCl and AgCl solution, Radiometer Analytical) were used as the counter and reference electrodes, respectively. The electrodeposition was carried out at a constant voltage of 1.3 V_{NHE} (1.7 V_{RHE}) for 15 minutes.

Photoelectrochemical characterization was carried out using the same three-electrode configuration. The electrolyte used is an aqueous 0.5 M K_2SO_4 (99%, Alfa Aesar) solution buffered to pH ~5.6 with K_2HPO_4/KH_2PO_4. The light source is a Newport Sol3A Class AAA Solar Simulator (type 94023A-SR3) that provides simulated AM1.5 illumination (100 mW/cm^2).

Photochemical stability measurements were performed using monoclinic $BiVO_4$ powder (Ciba Specialty Chemicals), with a typical particle size of 200-500 nm. This powder was dispersed in aqueous solutions with a pH ranging from 1 - 13 (adjusted using HCl/KOH), and

stirred for 24 hours with and without UV-illumination. The solutions were subsequently centrifuged to remove the powder, and the Bi and V contents of the supernatant were analyzed using inductively-coupled plasma optical emission spectroscopy (ICP-OES).

RESULTS AND DISCUSSION

Figure 2a shows a photograph of a 100 nm $BiVO_4$ film on FTO substrate (left) next to a bare FTO substrate (right). The yellow color indicates the presence of $BiVO_4$, and only a small amount of light scattering is shown by the sample. The microstructure of the film is characterized using planar and cross-sectional SEM, as shown in Fig. 2b and c, respectively. A typical particle size of ~100 nm is obtained, which is much smaller than that of earlier samples prepared by less well-defined glass spray nozzles [9].

Photochemical stability of $BiVO_4$

The stability of $BiVO_4$ in solutions of different pH, with and without illumination, is shown in Figure 2d.The material is found to be stable between pH 3 and 11, both in the dark and under UV illumination. Under both acidic (pH < 3) and alkaline (pH > 11) conditions the vanadium dissolves preferentially, exceeding the amount of dissolved bismuth by a factor of ~100. At pH 1 the dissolution rate is much higher under illumination than in the dark, whereas the dark- and photo-corrosion rates are approximately equal under alkaline conditions.

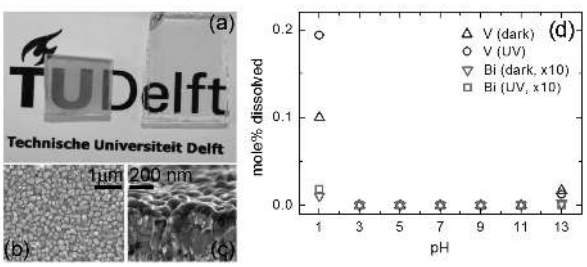

Figure 2. (a) Photograph of 100 nm thick $BiVO_4$ on an FTO-substrate (left) and a bare FTO-substrate (right). (b) Planar, and (c) cross-section scanning electron microscopy image of 100 nm thick $BiVO_4$ sample. (d) Mole% of Bi (×10) and V dissolved after 24 hours in the dark and under UV illumination in aqueous KOH/HCl solutions of varying pH.

Photoelectrochemical characterization of thin film $BiVO_4$

Figure 3 shows the photocurrent-voltage curves of 200 nm-thick uncatalyzed and Co-Pi catalyzed $BiVO_4$ samples under chopped AM1.5 illumination. The $BiVO_4$ was illuminated via the substrate, i.e., the back-side. The uncatalyzed sample (black curve) shows a photocurrent of ~0.7 mA/cm^2 at 1.23 V vs. RHE. While this is higher than previous reported values for bare $BiVO_4$ [2-8], it is still a factor of 10 lower than the theoretical maximum photocurrent that can be achieved by $BiVO_4$ (7.5 mA/cm^2, assuming that all photons with energies >2.4 eV are absorbed). Based on previous reports on $BiVO_4$, slow water oxidation kinetics is the performance limiting

factor at this illumination intensity [4-8]. In order to overcome this, 30 nm Co-Pi catalyst is deposited on the surface of $BiVO_4$ photoanode. As a result, a photocurrent of ~1.8 mA/cm^2 at 1.23 V vs. RHE is achieved, as shown in Fig. 3 (red curve). This significant improvement illustrates the improved catalytic activity of the photoanode upon the application of a Co-Pi catalyst.

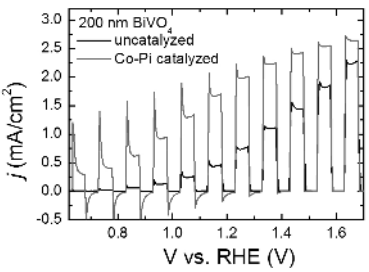

Figure 3. Chopped photocurrent-voltage measurement of uncatalyzed and Co-Pi catalyzed $BiVO_4$ of 200 nm thick under AM1.5 back-side illumination. The scan rate is 10 mV/s.

Despite the large enhancement of the catalytic activity for water oxidation, the red curve in Fig. 3 still shows pronounced photocurrent transients at potentials below ~1.2 V_{RHE}. We attribute this to sub-optimal coverage of the $BiVO_4$ with Co-Pi during the electrodeposition process. Further improvements may be possible by *photo*-deposition of the Co-Pi, which ensures that the Co-Pi is deposited at surface sites where the photo-generated holes are most readily available [12].

The photocurrent of Co-Pi catalyzed $BiVO_4$ is shown as a function of thickness in Figure 4a. A 300 nm $BiVO_4$ film gives the highest photocurrent of ~1.9 mA/cm^2 at 1.23 V vs. RHE under back-side illumination. This is one of the highest photocurrents ever reported for $BiVO_4$ catalyzed with a low-cost earth-abundant catalyst. A likely explanation for the optimum thickness is that thinner films absorb less light, whereas charge transport is limiting for thicker films. This is in agreement with a theoretical calculation of the optical absorption of $BiVO_4$ photoanodes based on its refractive index [13]. As shown in Figure 4b, the optical absorption remains nearly constant for films thicker than 300 nm.

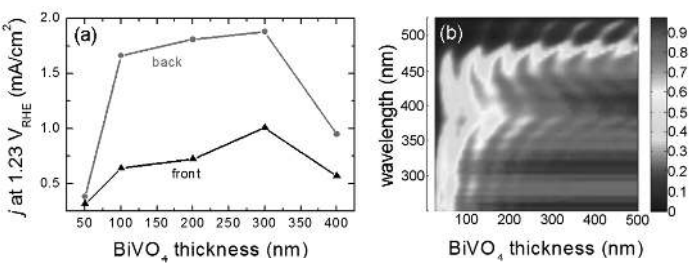

Figure 4. (a) AM1.5 photocurrent of $BiVO_4$ catalyzed with a 30 nm Co-Pi film as a function of the $BiVO_4$ thickness under front- and back-side illumination. (b) 2D color plot of the calculated absorption as a function of wavelength and $BiVO_4$ film thickness.

To further improve the performance of the films, it is important to first determine the performance-limiting factor of the Co-Pi catalyzed $BiVO_4$ photoanode. An elegant way to analyze the performance of a photoelectrode is recently reported by Dotan et al [14]. The total photocurrent due to water splitting can be described by the following equation:

$$J_{H_2O} = J_{abs} \times \eta_{sep} \times \eta_{ox} \quad (1)$$

where J_{abs} is the photon absorption rate expressed as a current, η_{sep} is the charge separation efficiency, and η_{ox} is the water oxidation efficiency. When hydrogen peroxide is added into the electrolyte solution, it acts as an effective hole scavenger. This results in a 100% oxidation efficiency ($\eta_{ox} = 1$), and the following equation can be written:

$$J_{H_2O_2} = J_{abs} \times \eta_{sep} \quad (2)$$

Based on equation (1) and (2), the charge separation efficiency and the oxidation efficiency can be obtained from the following equations:

$$\eta_{sep} = \frac{J_{H_2O_2}}{J_{abs}} \quad (3); \qquad \eta_{ox} = \frac{J_{H_2O}}{J_{H_2O_2}} \quad (4)$$

Figure 5a shows photocurrent-voltage curves of 100 nm thick $BiVO_4$ sample in a normal electrolyte (black curve) and in the presence of H_2O_2 (blue curve). The photocurrent of a Co-Pi catalyzed sample is also shown (red curve). Based on these curves, the oxidation efficiency and the charge separation efficiency of the samples have been calculated using Eqs. (3) and (4) and plotted in Figure 5b. The Co-Pi clearly enhances the oxidation efficiency of $BiVO_4$, reaching values >90% at potentials positive of 1.2 V_{RHE}.

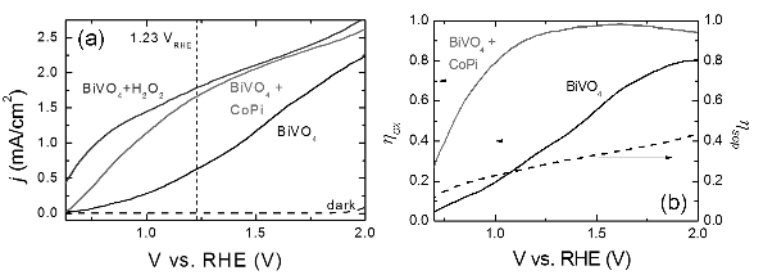

Figure 5. (a) AM1.5 photocurrent vs. voltage for a 100 nm $BiVO_4$ photoelectrode (with and without H_2O_2 in the electrolyte) and a Co-Pi catalyzed $BiVO_4$ photoelectrode at a scan rate of 50 mV/s. The dark curve is shown by the horizontal black dashed line. (b) Oxidation and charge separation efficiencies of uncatalyzed and Co-Pi catalyzed $BiVO_4$ as a function of applied bias.

Fig. 5b shows that the charge separation efficiency is the main problem to be addressed. About 60-80% of the electron-hole pairs recombine before reaching the interfaces. A pronounced